Journal Pre-proofs

Design and development of a chitosan-based nasal powder of dimethyl fumarate-cyclodextrin binary systems aimed at nose-to-brain administration. A stability study

Eleonora Sofia Cama, Laura Catenacci, Sara Perteghella, Milena Sorrenti, Mino R. Caira, Giovanna Rassu, Elisabetta Gavini, Paolo Giunchedi, Maria Cristina Bonferoni

PII: S0378-5173(24)00450-2
DOI: https://doi.org/10.1016/j.ijpharm.2024.124216
Reference: IJP 124216

To appear in: *International Journal of Pharmaceutics*

Received Date: 26 January 2024
Revised Date: 6 May 2024
Accepted Date: 7 May 2024

Please cite this article as: E. Sofia Cama, L. Catenacci, S. Perteghella, M. Sorrenti, M.R. Caira, G. Rassu, E. Gavini, P. Giunchedi, M. Cristina Bonferoni, Design and development of a chitosan-based nasal powder of dimethyl fumarate-cyclodextrin binary systems aimed at nose-to-brain administration. A stability study, *International Journal of Pharmaceutics* (2024), doi: https://doi.org/10.1016/j.ijpharm.2024.124216

Design and development of a chitosan-based nasal powder of dimethyl fumarate-cyclodextrin binary systems aimed at nose-to-brain administration. A stability study.

Eleonora Sofia Cama[1], Laura Catenacci[1], Sara Perteghella[1], Milena Sorrenti[1*], Mino R. Caira[2], Giovanna Rassu[3], Elisabetta Gavini[3], Paolo Giunchedi[3], Maria Cristina Bonferoni[1]

[1]Department of Drug Sciences, University of Pavia, 27100 Pavia, Italy.
[2]Department of Chemistry, University of Cape Town, 7701 Rondebosch, South Africa.
[3]Department of Medicine, Surgery and Pharmacy, University of Sassari, 07100 Sassari, Italy

[*]Corresponding authors.
E-mail addresses: milena.sorrenti@unipv.it (M. Sorrenti)

Abstract
The nasal administration route has been studied for the delivery of active molecules directed to the Central Nervous System, thanks to the anatomical connection between the nasal cavity and the brain.
Dimethyl fumarate is used to treat relapsing-remitting multiple sclerosis, with a role as an immunomodulator towards T-T-cells and a cytoprotector towards neurons and glial cells. Its use in therapy is hindered by its low aqueous solubility, and low stability, due to hydrolysis and sublimation at room temperature. To overcome this limitation, in this study we evaluated the feasibility of using two amorphous β-cyclodextrin derivatives, namely hydroxypropyl β-cyclodextrin and methyl β-cyclodextrin, to obtain a nasally administrable powder with a view to nose-to-brain administration.
Initially, the interaction product was studied using different analytical methods (differential scanning calorimetry, Fourier transform infrared spectroscopy and powder X-ray diffraction) to detect the occurrence of binary product formation, while phase solubility analysis was used to probe the complexation in solution.
The dimethyl fumarate-cyclodextrin binary product showing best solubility and stability properties was subsequently used in the development of a chitosan-based mucoadhesive nasally administrable powder comparing different preparative methods. The best performance in terms of both hydrolytic stability and DMF recovery was achieved by the powder obtained via freeze-drying.

Keywords
Nasal powder, dimethyl fumarate, cyclodextrin, nose-to-brain, multiple sclerosis

1. INTRODUCTION
Dimethyl fumarate (DMF) is an α,β-unsaturated ester (dimethyl ester of fumaric acid), first isolated from the roots of Fumaria officinalis, that has been approved for the treatment of plaque psoriasis, under the name of Fumaderm® (Mrowietz et al., 2017), and nowadays used as capsules to treat relapsing-remitting multiple sclerosis (RRMS), a chronic autoimmune, inflammatory disorder of the Central Nervous System (CNS). Two placebo-controlled phase III studies, DEFINE and CONFIRM, demonstrated the clinical efficacy of DMF against RRMS over 2 years (Havrdova et al., 2013). RRMS is the most common form of multiple sclerosis, affecting about 85% of MS patients. It is characterized by flare-ups (relapses) of symptoms followed by periods of remission when symptoms improve or disappear (Goldenberg, 2012). RRMS is, already in early stages, characterized by inflammation, demyelination, and axonal loss, with a typical onset between the age of 20 and 40 years, more frequently in women than men, and with a development that can be extremely different among the individual patients (McGinley et al., 2021). DMF is available as capsules for oral administration, commercialized under the name Tecfidera®, and authorized by the Food and Drug Administration (FDA) in 2013 and by the European Medicines Agency (EMA) in 2014 (Dello Russo et al., 2021). However, its complete mechanism of action is still unclear; DMF may have both an immunomodulatory effect towards T-cells (involved in the inflammatory process) and a cytoprotective effect towards neurons and glial cells, through the activation of Nrf2-mediated or HCAR2-mediated signalling pathways (Linker and Haghikia, 2016).
In the gastrointestinal (GI) tract, the esterases rapidly cleave DMF into monomethyl fumarate (MMF), its primary active metabolite, which reaches its peak concentration 2-2.5 hours after ingestion. MMF is subsequently metabolized in the bloodstream into fumaric acid (FA), which enters the Krebs cycle and is eventually eliminated via breathing, since it is metabolized into carbon dioxide and water. This is the primary excretion pathway of DMF (about 60% of the dose), whereas a small amount is eliminated through urine and faeces (Linker and Gold, 2013; Linker and Haghikia, 2016). DMF presents some collateral effects, mainly associated with the gastrointestinal tract (diarrhea, nausea, abdominal pain, vomiting) (Linker and Gold, 2013). Moreover, it shows limited water solubility and low stability, due to hydrolysis and sublimation at room temperature (Guzowski et al., 2016; Kawakami et al., 2011).
To overcome the limitation of DMF stability, in the present study, the feasibility of the use of cyclodextrins (CDs) has been investigated, according to their stabilizing effect described in the literature (Popielec and Loftsson, 2017). The CDs are natural oligosaccharides that can be useful as excipients for their capability to act as solubilizers and absorption

enhancers (Giunchedi et al., 2020; Gänger and Schindowski, 2018; Jansook et al., 2018). CDs, with their unique toroidal shape formed by glucose units, exhibit a versatile capacity to create inclusion complexes by encapsulating guest molecules within their central cavity through non-covalent interactions, as they feature a hydrophilic exterior and a hydrophobic interior cavity, enabling them to selectively host a diverse array of compounds. In particular, for this objective, the semisynthetic derivatives most widely used in the pharmaceutical field are 2-hydroxypropyl-β-CD (HPβCD), heptakis(2,6-di-*O*-methyl)-β-CD (DMβCD/DIMEB), sulfobutylether sodium salt β-CD (SBEβCD) and randomly methylated β-CD (RMβCD/RAMEB) (Jansook et al., 2018). In our previous studies, natural and derivatized cyclodextrins were used to improve the solubility and the stability of some antioxidant bioactive compounds such as resveratrol and pterostilbene. The interaction between the two components was achieved through different complexation methods, both in solution and in the solid state and was widely investigated by thermal analysis, FTIR spectroscopy and phase solubility studies (Catenacci et al., 2020; Catenacci et al., 2022; Catenacci et al., 2023).

In recent years, the nasal administration route, especially owing to the anatomical connection between the nasal cavity and the brain, has been extensively studied for drugs and biologically active molecules directed to the CNS (Bonferoni et al., 2020; Chapman et al., 2013). In fact, 95% of molecules cannot cross the blood brain barrier (BBB), so they are not able to reach the brain in the appropriate concentration needed to treat neurological diseases. The nose-to-brain (N2B) drug delivery route seems to be a good alternative to overcome this challenge, as the drugs can reach the cerebrospinal fluid through two pathways: the extracellular and the intracellular pathway, involving the olfactory and trigeminal nerves (Gänger and Schindowski, 2018).

Quite recently the possibilities related to N2B delivery have been explored for drugs approved for MS treatment, such as IFN-β, teriflunomide, fingolimod and methylprednisolone (Mwema et al., 2023). However, relatively little investigation into the possible N2B delivery of anti-MS drugs in general, and DMF in particular, has been reported, possibly also due to some challenges related to its low stability. It is possible to mention a study in which DMF was encapsulated in solid lipid nanoparticles (SLNs) and administered to mice by the intraperitoneal and intranasal routes (Esposito et al., 2017).

Recently, CDs have also been investigated as possible excipients for nasal drug delivery, and several examples can be cited regarding the use of CDs as solubilizers and absorption promoters (Rassu et al., 2021; Truzzi et al., 2021). Luppi et al. investigated nasal formulations of tacrine, used to treat Alzheimer's disease, obtained using albumin nanoparticles carrying β-CD and its two derivatives HPβCD and SBEβCD: the drug's permeation rate was thus increased ex vivo, and the CDs had the ability to modulate the drug loading and mucoadhesion (Luppi et al., 2011). Furthermore, according to Manta et al., not only were quercetin's water solubility and stability increased after complexation with RAMEB and HPβCD, but also permeation across rabbit nasal mucosa was higher, leading to a detectable concentration of the drug in the brain after nasal powder administration compared to the oral route (Manta et al., 2020). Spherical methyl-β-cyclodextrin microparticles loaded with deferoxamine mesylate were obtained by Rassu et al. showing that the CD can enhance the drug permeation across neuron-like monolayers (Rassu et al., 2015).

In this study, in particular, we investigated the possibility of complexation between DMF and some derivatives of β-CD, such as HPβCD and RAMEB, to improve the DMF solubility and stability, with a view to N2B administration. The loading of DMF in micro or nanocarriers and in nasal powders in fact involve several steps, such as solubilisation, heating, drying or solvent evaporation, that potentially expose the drug to sublimation and degradation by hydrolysis. Considering this drug's instability, as a preparative method to complex the drug with CDs, kneading was selected as more convenient in this respect. The most promising API-CD binary system was subsequently characterized and investigated, to obtain a chitosan-based mucoadhesive nasal powder via different preparative methods. Particular attention was given to DMF mass recovery and to the occurrence of hydrolytic derivatives during the powder preparation.

2. MATERIALS AND METHODS

2.1 Materials

Dimethyl fumarate (DMF, 99%) was purchased from AK Scientific Inc. (Union City, USA). Monomethyl fumarate (MMF, 97%) and fumaric acid (FA, 99%) were purchased from Sigma Aldrich, Co (St Louis, MO, USA). Hydroxypropyl-β-cyclodextrin (HPβCD, Mw: 1,400 g/mol) was a gift from Cyclolab Ltd. (Budapest, Hungary). Randomly methylated β-cyclodextrin (RAMEB, Cavasol® W7 M Pharma, Mw: 1,302 g/mol) was purchased from Wacker-Chemie Italia (Peschiera Borromeo, Milan, IT). Mannitol was purchased from Roquette Italia (Cassano Spinola, Alessandria, IT). Chitosan-HCl (CS·HCl), Tripolyphosphate sodium, Agar and Gastrin mucin porcine type III were purchased from Sigma Aldrich (Milan, IT). Ultrapure water was obtained from a MilliQ® apparatus (Millipore, USA). Methanol of chromatographic grade was acquired from PanReac® AppliChem® (ITW Reagents®, Darmstadt, Germany).

2.2 Methods

2.2.1 Sample Preparation

Physical mixtures (PMs)

For the preparation of homogeneous PMs, DMF + HPβCD and DMF + RAMEB, the powders were sieved separately to obtain a particle size fraction <250 μm. The sieved powders of DMF and each CD, in 1:1 and 1:2 molar ratio, respectively, were mixed in a Turbula mixer at ~60 rpm for 30 minutes.

Kneading (KN)
About 1 g of each DMF-CD PM was wetted with a minimum amount of ethanol (≈0.4 mL) in a mortar to obtain a soft paste that was then dried to a constant mass at room temperature. This procedure was repeated three times and the samples were finally sieved (<250 μm).

2.2.2 Phase solubility analysis
The increase in the aqueous solubility of DMF, through the complexation with CDs, was achieved using the method described by Higuchi and Connors (Higuchi, 1965).
Each CD was dissolved in phosphate buffered saline solution (PBS) with a pH of 7.4, as representative of physiological conditions, albeit in the upper range of nasal pH (Kim et al., 2013). Solutions were obtained with concentrations in the range 0–200 mM for HPβCD and 0-100 mM for RAMEB. An excess of DMF (~140 mg) was added to 5 mL of each CD solution. The solutions were placed under mechanical shaking, in a temperature-controlled water bath (T = 25 ± 1 °C) until equilibrium was reached (24 h). Aliquots of these solutions were then filtered using 0.22 μm Millipore nitrocellulose filters, and the concentration of DMF was determined by HPLC (2.2.3).

2.2.3 HPLC determination of DMF and its metabolites
DMF, MMF and FA have been quantified by HPLC (Habib et al., 2021). The analyses were performed using a chromatographic system consisting of an Agilent 1100 binary pump, an ALS sampler with a VWD UV-VIS detector. The mobile phase consisted of methanol and water solution with phosphoric acid 0.1% (55:45 (v/v); pH = 2.5). Analytes were separated using an RP-18 endcapped column, 150 mm x 4.6 mm, 3 μm i.d. (Merck KGaA). The workflow was 0.5 mL/min and the injection volume was 20 μL. The detector was set to a wavelength of 210 nm. The duration of the chromatographic run was 8 minutes per sample.
The assay was linear in the concentration range 5-50 μg/mL (DMF: y = 279094x – 134.71; R^2 = 0.9935. MMF: y = 284464x – 182.82; R^2 = 0.9964. FA: y = 290158x – 70.797; R^2 = 0.9997).

2.2.4 Stability studies
The chemical stabilities of DMF and its binary systems with CDs, both as a powder and in aqueous solution, were evaluated. Adequate amounts of powder samples were stored at 25 ± 2 °C in the laboratory atmosphere while the solutions were stored at 4 ± 2 °C in the refrigerator.
The determination of the concentration of DMF in the samples was carried out by HPLC at different set times: 0, 1, 2, 7 and 14 days respectively. For each point and sample, three measurements were performed, and the results were reported as mean ± SD.

2.2.5 Freeze drying process
The KN products were solubilized both in an aqueous solution and in a mannitol aqueous solution (5% w/v) and subjected to freezing at −20 °C for 24 h and then to sublimation for 48 h in an Epsilon 2-4 LSCplus Pilot freeze dryer.

2.2.6 Design of Experiment
A Full Factorial 2^3 Design of Experiment (DoE) approach was used to evaluate the influence of formulative factors on the recovery of DMF after a freeze-drying process. X1 was the type of CD used to prepare the product, HPβCD and RAMEB (-1 and +1 level respectively); X2 was the stoichiometric molar ratio between DMF and each CD set at 1:1 to 1:2 (-1 and +1 level respectively); X3 was the amount of mannitol in the freeze-dried product, selected at zero and at 5% (w/v) (-1 and +1 level respectively). The design involved a total of 8 experiments and was entirely duplicated. Two more samples, consisting of DMF solutions without CD, with and without 5% w/v mannitol, were prepared as control and processed together with the samples of the experimental design.
In the choice of the response, the results obtained with uncomplexed DMF were taken into account.

Response DMFCD/DMFfree, was calculated as the ratio between the % recovery of total DMF when complexed with CD, to the % recovery of total DMF in control (without CD) samples:

$$\frac{DMFCD}{DMFfree} = \frac{DMF_{recovered} in\ DMF{-}CD}{DMF_{recovered} in\ control} \text{ (Eq. 1)}$$

Response MMF/DMF was the ratio between μmol of MMF and of DMF in complexed samples.

$$\frac{MMF}{DMF} = \frac{\mu moles_{MMF}}{\mu moles_{DMF}} \text{ (Eq. 2)}$$

Response MMFCD/MMFfree was the ratio between the % recovery of MMF in samples complexed with CD and the % of μmol of MMF found in control samples containing free drug (without CD).

$$\frac{MMFCD}{DMFfree} = \frac{MMF_{recovered} inCD}{MMF_{recovered} in\ control} \text{ (Eq. 3)}$$

The data were elaborated with the statistical software package Statgraphics Centurion18 Technologies, The Plains, Virginia.

2.2.7 Physicochemical characterization

Thermal analysis

For the thermal characterization of DMF-CD binary products, Differential Scanning Calorimetry (DSC) analyses were performed on a Mettler STAR^e system (Mettler Toledo, Milan, Italy) equipped with a DSC821^e Module and an Intracooler device for sub-ambient temperature analysis (Julabo FT 900, Seelbach, Germany). Samples of 2–4 mg were weighed on a Mettler M3 Microbalance, placed in sealed aluminium pans with pierced lids and analyzed in the temperature range 30–350 °C (heating rate β = 10 K min^{-1}, N_2 atmosphere with a flow rate of 50 mL min^{-1}). The instrument was previously calibrated with indium as a standard reference, and the analyses were measured at least in triplicate.

A Mettler STAR^e TGA system with simultaneous DSC (TGA/DSC1) (Mettler Toledo, Milan, Italy) was used to measure the mass losses. 3–4 mg samples were placed in alumina crucibles with pierced lids under the same experimental conditions used for DSC, and again the instrument was calibrated with indium as a standard reference. The measurements were performed at least in triplicate.

Fourier Transform Infrared spectroscopy

Fourier Transform Infrared (FT-IR) mid-IR spectroscopy (650–4000 cm^{-1}) was performed on a Spectrum One spectrophotometer (64 scans with a resolution of 4 cm^{-1}) (Perkin Elmer, Monza, Italy) equipped with a MIRacle™ ATR device (Pike Technologies, Madison, Wisconsin, USA). The untreated samples were pressed on an ATR crystal of ZnSe for the acquisition of the spectrum in transmittance mode, and the spectra were collected at least in triplicate.

Powder X-ray diffraction

A D5005 Bruker model diffractometer (Bruker, Germany), with a graphite monochromator and a scintillation detector, was used. Measurements were collected using CuKα_1 radiation (λ = 1.5406 Å, Coolidge tube). The data acquisitions were recorded at ambient temperature, in the angular range $4 < °2\theta < 40$, with step size 0.02° and an acquisition time of 10 s.

Scanning electron microscopy

Scanning electron microscopy (SEM) images were acquired at room temperature by using a high-resolution FE-SEM scanning electron microscope (Tescan Mira3 XMU series, Brno-Kohoutovice, Czech Republic); a high voltage (20 kV) and a high vacuum (6 x 10^2 Pa) were applied.

Optical microscopy and particle size distribution

Microscopic observation of samples was performed with an Inverted optical Microscope BDS400 (TiEsseLab, Milan, IT) at 20× magnification. Particle size distribution was obtained from the optical microscope images, by means of ImageJ software (Schneider et al., 2012) on about 300 particles, using the Martin's diameter (Mukesh et al., 2021).

2.2.8 Preparation of chitosan-based nasal powder

For every powder obtained, drug loading % and recovery % were calculated. In particular:

- *Drug Loading (DL%)* is defined as the ratio between the amount of drug in mg recovered in the formulation ($DMF_{recovered}$) and the amount of powder in mg (M_{powder}):

$$DL\% = \frac{DMF_{recovered}}{M_{powder}} \times 100 \qquad \text{(Eq. 4)}$$

- *Percentage recovery* is expressed as the amount of drug recovered as a result of a production process that may lead to a loss of active ingredient; it is defined as the ratio between the amount of DMF recovered ($C_{recovered}$) at the end of the process and the total amount of theoretical active ingredient, present in the starting solution ($C_{solution}$):

$$Recovery\% = \frac{C_{recovered}}{C_{solution}} \times 100 \qquad \text{(Eq. 5)}$$

Spray drying

To prepare a dry nasal powder based on chitosan·HCl (CS·HCl), a spray drying method was employed [21]. Firstly, CS·HCl 1% (w/v) was solubilized in 50 mL of water, and subsequently, the powders of pure DMF and DMF-RAMEB 1:2 (mol/mol) KN product (70 and 500 mg, respectively) were added to their respective CS·HCl solutions. A spray dryer "BUCHI Mini Spray Dryer B-191" was used, with an inlet temperature of 120 °C, spray rate of 8 mL/min, aspiration of 70%, and flux of 400-600 L/h.

Ionotropic gelation

The ionotropic crosslinking method has been widely proposed in the literature for the preparation of chitosan-based beads and nanoparticles (Dehghan et al., 2013; Jarudilokkul et al., 2011; Mazancová et al., 2018; Wilson et al., 2021). An amount of DMF-RAMEB KN product was added to a CS·HCl solution (1 g/100 mL; pH = 4.5) at T= 20 ± 2 °C, under magnetic stirring until complete solubilization was reached. The sodium tripolyphosphate (TPP) solution (2 g/100 mL) was prepared by solubilizing the TPP in distilled water under magnetic stirring at 500 rpm and adjusted with hydrochloric acid to pH = 4.8. The CS·HCl solution was subsequently added dropwise into the TPP solution, producing beads, and then separated by centrifugation at 1500 rpm for 6 min and subsequently washed with water and resuspended in PBS (pH = 7.4).

The addition of magnetic stirring at 1500 rpm while dripping the CS·HCl solution into the TPP solution led to the formation of nanospheres. The suspension was dialyzed with a tubular dialysis cellulose membrane with a cut-off of 14 kDa.

The obtained products were both subjected to a process of freeze drying to obtain powders.

Freeze drying

Freeze dried solutions of the most promising KN product (DMF-RAMEB 1:2, corresponding to a DMF concentration of 1.4 mg/ml) with CS·HCl (1%) were prepared, in 1 mL glass vials.
After complete solubilization, all the samples in the vials were subjected to a freeze drying process (Epsilon 2-4 LSCplus Pilot Freeze Dryers).

2.2.9 Water Uptake

The investigation of water uptake capability was carried out by the modified Enslin apparatus as previously described (Rassu et al., 2018). Powder (10 mg) was uniformly dispersed on a cellulose filter disk saturated with MilliQ water, lying on the top of a fritted glass support, connected with a graduated capillary. The volume of water absorbed (μL) during the time interval from 0.25 up to 30 min was measured. The result is the average of three determinations (n = 3; ± SD).

2.2.10 Mucoadhesion test

The mucoadhesion of the powder obtained by freeze drying was evaluated in vitro by determining the adhesion force of each powder on agar gel, with or without mucin, distributed on an inclined plane (Trenkel and Scherliess, 2021).
A hot solution of 1.5% agar with or without mucin (1% w/w) in PBS (pH 6.4, Ph. Eur.), was cast on a petri dish (diameter 5.5 cm) and stored for 30 min at T = 25 ± 2 °C. To evaluate the adhesion force, the petri dishes were placed in an upright position with an angle of 45°. 15 mg of powder per sample was placed on the top of the gel in a spot with a diameter of approximately 5 mm and the displacement of the powder samples was measured as a function of time. For each formulation, the assays were performed in triplicate.
Mucoadhesive strength was evaluated ex vivo by a modified precision balance (Juliano et al., 2008) using excised nasal mucosa from pigs. The mucosa was attached on the base of the balance and re-hydrated with artificial nasal mucus, containing 8% (w/v) of mucin type II from the porcine stomach (Sigma-Aldrich, Milan, Italy) in a solution of NaCl (7.45 mg/mL), KCl (1.29 mg/mL) and $CaCl_2 \cdot 2H_2O$ (0.32 mg/mL) (Colombo et al., 2018). The powder was layered on the double-sided adhesive tape and fixed on the top of the instrument. The two parts were then put in contact, and a contact force of 15 g was maintained for 150 s; afterwards, the strength (g) needed for the complete detachment was measured. As control, the test was also performed using double-sided adhesive tape alone. The mucoadhesive strength was calculated and expressed in N/cm^2. The experiments were performed in triplicate (n=3).

3. RESULTS AND DISCUSSION

3.1 Phase solubility analysis

In Figure 1, the phase solubility results obtained by plotting the apparent equilibrium DMF concentration versus the concentrations of the CD employed in the experiment are shown. For both CDs, the profiles were of A_L type with a linear increase of drug solubility with increasing CD concentration, because of the soluble complex formation.

In particular, the solubility of the drug was increased 3-fold, both at the maximum concentrations of HPβCD (200 mM) and RAMEB (100 mM) employed.

Figure 1. Phase solubility diagram of DMF as a function of [HPβCD] (red) and [RAMEB](blue).

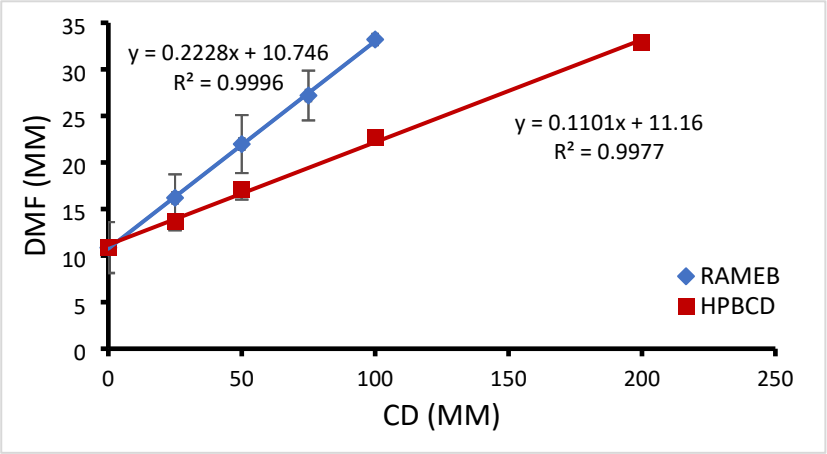

The apparent stability constant $K_{1:1}$ of the complexes was estimated using the following equation:

$$K_{1:1} = \frac{slope}{S_0(1-slope)} \qquad \text{(Eq. 6)}$$

where S_0 is the DMF solubility in aqueous solution (Esposito et al., 2017) in the absence of CD (11.35 mM) and slope is calculated from the straight-line portions of the recorded diagrams.

The 1:1 apparent stability constants of the complexes formed with HPβCD, and RAMEB were 11.4 and 26.4 M^{-1}, respectively, indicating relatively weak interactions between DMF and these derivatized CDs.

3.2 Stability studies

The sublimation behaviour of DMF alone and in combination with CDs was analysed by a preliminary stability test, evaluating the concentration of the drug and its degradation products, MMF and FA, in solid and solution samples.

In Figure 2 the stability results of an aqueous ~~methanol~~ solution of DMF (1.4 mg/ml) stored at 4 ± 1 °C, assumed as reference, are shown. After 14 days the DMF concentration decreased by about 16%, with a consequent increase of MMF, the active metabolite, concentration (≈14%) and, for a small part, into FA (≈2.7%).

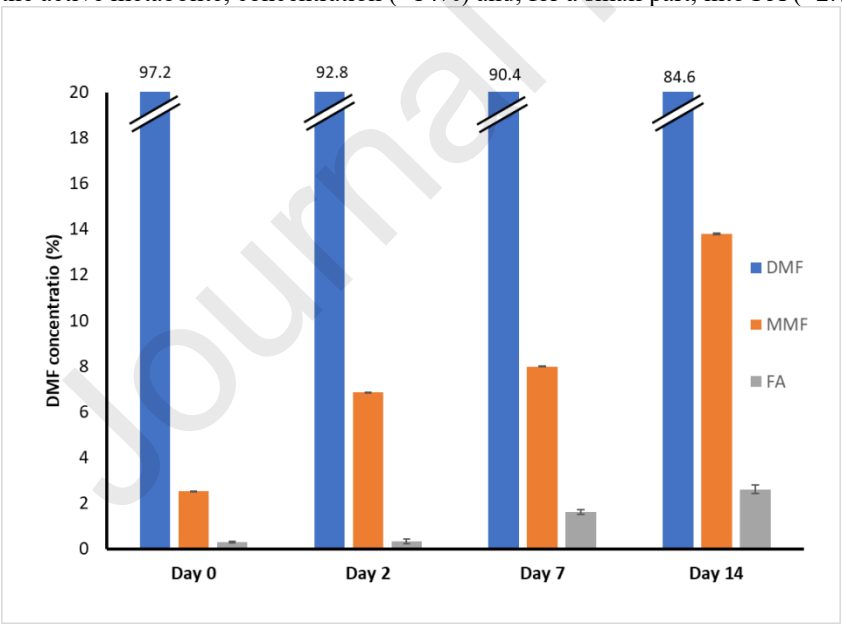

Figure 2. ~~Stability~~ Concentration of commercial DMF in solution at time 0 and after storage for 2, 7 and 14 days at 4 ± 1 °C.

3.2.1 DMF-HPβCD binary system

In Figures 3a and 3b the stability studies of the same KN products in the solid state and in solution are shown.

The percentage of DMF in the KN products stored at 2~~0~~5 ± 2 °C with HPβCD remained stable for 14 days (from ~96% at t_0 to ~95% at 14 days), with a concentration of the inactive FA less than 0.7%, regardless of the molar ratio between the active and the CD.

The DMF concentration in the DMF-HPβCD equimolar system was reduced by about 12% with a greater presence in the sample of MMF. However, the lower concentration of FA (~0.5%) could be attributed to the stabilizing effect due to the presence of HPβCD in the system. The concentration of the inactive metabolite was even lower in the KN product with the higher CD concentration, confirming that the presence of CD in solution makes the drug more stable to degradation into FA.

3.2.2 DMF-RAMEB binary system

The same stability studies were also carried out for the KN products of DMF with RAMEB and, as an example, the obtained results are shown in Figure 3.

As was observed for the other CD derivative, the presence of the CD stabilized the active, reducing the percentage of MMF and FA. In particular, after 14 days the DMF concentration remained higher than 92%, showing a greater stabilizing effect of RAMEB in comparison to the hydroxypropyl derivative. The best stabilizing effect was observed for the DMF-RAMEB 1:2 (mol/mol) system in solution, in which the percentage of DMF decreased by just over 1% with respect to the DMF initial value.

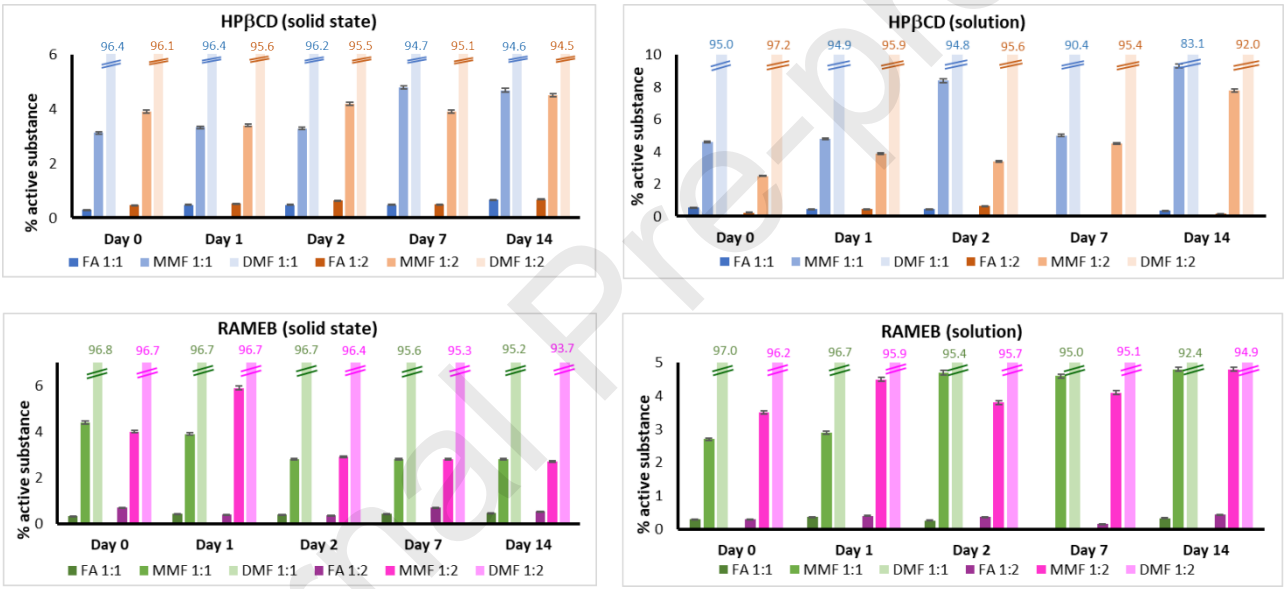

Figure 3. Concentration of active in the DMF-CD binary systems in the solid state and in solution at time 0 and after storage for 1, 2, 7 and 14 days at 25 ± 2 °C. ~~Stability of the DMF-CD binary systems in the solid state and in solution.~~

3.3 Freeze drying recovery studies and DoE

Given the tendency of DMF to sublime, several production processes of pharmaceutical formulations, including freeze drying and spray drying, could result in a major loss in titer. It was therefore verified whether the complexation with CDs resulted in a stabilizing effect against DMF sublimation, improving the DMF recovery in the final product. A freeze drying process was selected, as a particularly challenging method, to evaluate its effect on drug recovery in DMF-CD binary systems. The freeze dried samples were analyzed by HPLC, to determine the concentration of DMF, the presence of MMF (its active metabolite) and FA as the drug degradation product.

Each DMF-CD product, with HPβCD and RAMEB, in the stoichiometric ratios 1:1 (mol/mol) and 1:2 (mol/mol), in aqueous solution and in solution with mannitol, was prepared in duplicate. This corresponds to a full factorial design experiment with three factors and two levels, as described in the Methods section (section 2.2.6). Corresponding solutions of DMF without CD were processed in duplicate together with the DoE samples.

Figure 4 shows the results obtained in terms of the residual percentage of DMF, MMF and FA recovered after freeze drying as percentage of the initial amount (expected), for each of the processed samples.

Figure 4. Results expressed as µmoles found in freeze dried samples/expected µmoles (mean ± SD of three readings. Results for two different independent series are indicated as A and B).

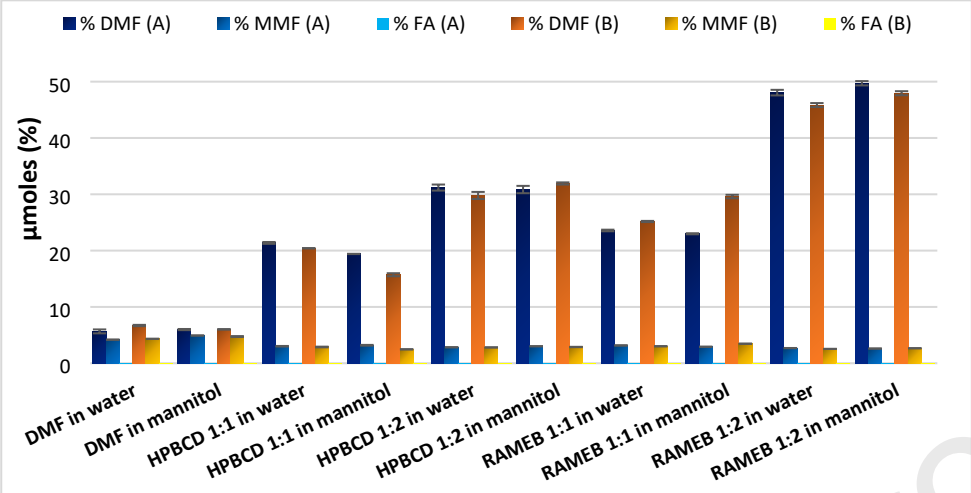

Considering the recovery of DMF, the analysis of the free DMF samples assumed as controls (DMF in water and DMF in mannitol), showed the almost total loss of the drug, reasonably due to sublimation, following the freeze drying process. Even considering the total µmoles of both DMF and MMF, it is possible to see that in these cases the mass loss was almost 90% of the initial drug present.

In all systems prepared with CDs, the DMF percentage found after freeze drying is higher than in the controls, ranging from 15 to 21% for DMF-HPβCD 1:1 (mol/mol) and between 29 and 31% for DMF-HPβCD 1:2 (mol/mol) KN products, respectively.

When the CD used was RAMEB, the amount of DMF recovered was even higher, and the best performance was achieved with the KN product containing the highest amount of CD (recovered DMF values between 45 and 49%).

The differences found between the different samples processed were analyzed by a Full Factorial Design, in which the type of CD, the molar ratio DMF-CD and the presence or absence of mannitol were considered as factors. The design used is described in the Methods section (section 2.2.6).

For the DMFCD/DMFfree response, the results of the variance analysis are shown in Table 1, while in Figure 5 the Pareto Chart and the plot of the statistically significant interaction, between CD and molar ratio, are given.

Table 1. Variance analysis for DMFCD/DMF free response.

Source	*Sum of Squares*	*Df*	*Mean Square*	*F-Ratio*	*P-Value*
A:CD	6.05273	1	6.05273	118.20	0.0000
B:ratio	13.3477	1	13.3477	260.67	0.0000
C:mannitol	0.0404794	1	0.0404794	0.79	0.3971
AB	1.32997	1	1.32997	25.97	0.0006
AC	0.127025	1	0.127025	2.48	0.1497
BC	0.066372	1	0.066372	1.30	0.2843
Total error	0.460851	9	0.0512057		
Total (corr.)	21.4252	15			

R-squared = 97.849 percent

R-squared (adjusted for d.f.) = 96.415 percent

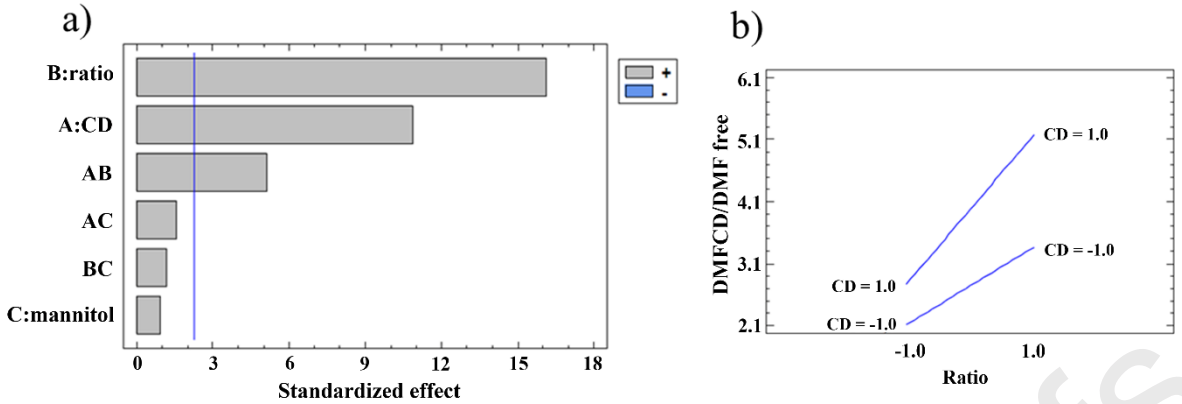

Figure 5. a) Pareto chart showing the effects of primary factors and binary interactions between the factors, and b) interaction graphs between ratio (DMF-CD) and type of CD.

As can be seen from the Variance Analysis table and the Pareto Chart (Figure 5a), two primary factors show statistically significant ($P<0.01$) influence on the response: the molar ratio between DMF and CD, and the type of CD used. Both the effects are positive. As for the molar ratio, therefore, with the 1:2 ratio, in which the complex involves a greater concentration of CD, a higher recovery of DMF than the 1:1 ratio was obtained. The type of CD used also appears to have a highly significant effect ($P<0.01$) on stabilization, clearly indicating that RAMEB stabilizes more effectively than HPβCD.

As can be seen from the variance analysis table and the Pareto Chart, the interaction between these factors is also highly significant ($P<0.01$). The interaction graph is shown in Figure 5b and shows that in the case of RAMEB, the stabilization following the increase in the molar ratio from 1:1 (mol/mol) to 1:2 (mol/mol) is more marked than in the case of HPβCD. No significant effect was shown for the presence of mannitol in solution.

During the analyses carried out to determine the concentration of DMF, particular attention was paid to assessing the presence of FA, as a degradation impurity, coming from the hydrolysis of the ester groups of the active.

In all the samples the percentage of FA is very low in comparison with that of DMF, as can be appreciated from Figure 4, and the analysis of its values in DoE did not show any statistically significant relationship with the studied factors.

The percentages of active substance present in the same samples in the form of MMF were also evaluated. It should be remembered that MMF, unlike FA, is still pharmacologically active, although it represents the result of ~~a~~ the first step of hydrolysis. The analysis of MMF/DMF values gives results in line with those obtained for DMFCD/DMFfree.

As shown in Table 2 and Figure 6, the use of a 1:2 molar ratio (+1 level) for both CDs leads to a decrease in the response, therefore a lower MMF/DMF ratio, indicating that both CDs reduce not only the mass loss but also the hydrolysis of DMF, with a stabilization effect, higher for the higher amount of CD in the complex. The effect of the CD type is statistically significant too, confirming that the use of RAMEB leads to a lower response, with a smaller amount of MMF occurrence than the use of HPβCD. Also, in this case, the presence of mannitol resulted in a non-significant effect.

Table 2. Variance analysis for MMF/DMF response.

Source	*Sum of Squares*	*Df*	*Mean Square*	*F-Ratio*	*P-Value*
A:CD	42.2175	1	42.2175	115.74	0.0000
B:ratio	162.244	1	162.244	444.79	0.0000
C:mannitol	0.522006	1	0.522006	1.43	0.2622
AB	1.44601	1	1.44601	3.96	0.0777
AC	1.91131	1	1.91131	5.24	0.0478
BC	0.566256	1	0.566256	1.55	0.2442
Total error	3.28291	9	0.364767		
Total (corr.)	212.19	15			

R-squared = 98.4528 percent
R-squared (adjusted for d.f.) = 97.4214 percent

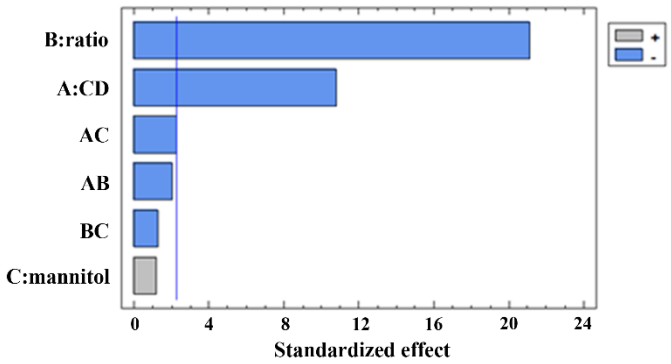

Figure 6. Pareto chart for the responses MMF/DMF.

In the Pareto chart of Figure 7 and the ANOVA results reported in Table 3, it is possible to see a similar effect even considering the response MMFCD/MMFfree.

Table 3. Analysis of Variance for the MMFCD/MMFfree response

Source	*Sum of Squares*	*Df*	*Mean Square*	*F-Ratio*	*P-Value*
A:CD	0.007396	1	0.007396	107.19	0.0000
B:ratio	0.0289	1	0.0289	418.84	0.0000
C:mannitol	0.001089	1	0.001089	15.78	0.0032
AB	0.000289	1	0.000144	4.19	0.0710
AC	0.000144	1	0.000009	2.09	0.1825
BC	0.000009	1	0.000069	0.13	0.7263
Total error	0.000621	9			
Total (corr.)	0.038448	15			

R-squared = 98.3848 percent
R-squared (adjusted for d.f.) = 97.3081 percent

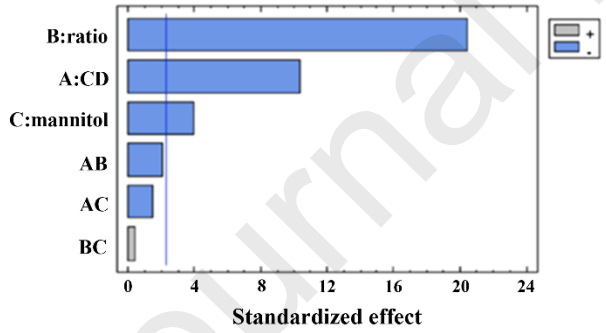

Figure 7. Pareto chart for the response MMFCD/MMFfree.

In this case, as for DMFCD/DMFfree, the stabilization effect of complexation is put in evidence by direct comparison with the samples without CD (controls). Highly significant effects of molar ratio and type of CD were observed also in this case, with better stabilization for RAMEB at 1:2 molar ratio. This is the only response for which a significant effect was seen for the presence of mannitol, which resulted in a slight reduction of DMF hydrolysis. It can be hypothesized that mannitol, as a cryoprotectant, reduces the availability of water for DMF hydrolysis.
All the results of the DoE study on the freeze dried samples indicate therefore that the complexation of DMF in CDs reduces the drug loss in mass during the freeze drying process, probably for the protection against sublimation. The susceptibility to hydrolysis too seems moreover clearly reduced by complexation in both CDs, and especially in this case for RAMEB at 1:2 molar ratio.

3.4 Physicochemical characterization of DMF and its binary system

3.4.1 Characterization of DMF

The commercial DMF is a white crystalline powder with a typical thermal profile of an anhydrous crystalline compound whose DSC (curve a) and TGA (curve b) profiles are shown in Figure 8. The DSC curve shows a single endothermic effect at T = 103.2 ± 0.7 °C related to the melting of the sample (T_{onset} = 100.5 ± 0.5 °C; ΔH_{melt} = 208 ± 2 J/g).

The anhydrous nature of DMF was confirmed by TGA analysis that shows a single mass loss at about 84 °C attributable to the decomposition of the melt.
These thermal parameters of the commercial DMF were used as references for the pure compound in the study of the interaction products with randomly methylated β-CD.

Figure 8. DSC (a) and TGA (b) curves and the FT-IR spectrum (c) of the commercial DMF.

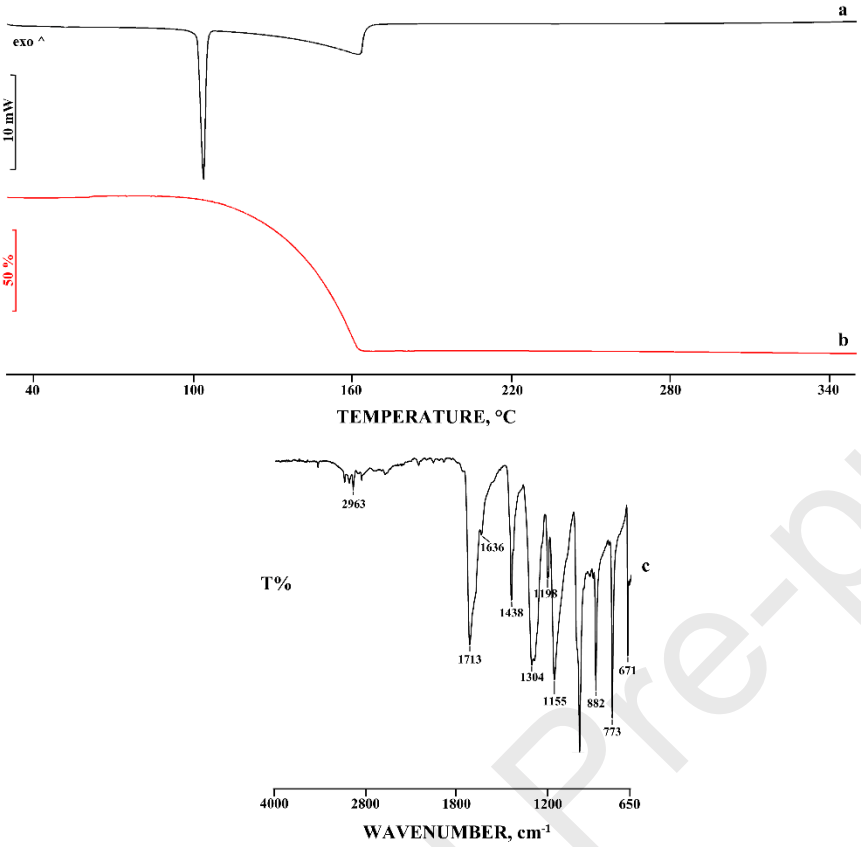

To further characterize the DMF solid-state, FT-IR analysis was carried out in the range between 4000 and 650 cm^{-1} and the spectrum obtained is reported in Figure 8 (spectrum c) in which the characteristic stretching and bending bands of the functional groups of the molecule were evident. In particular, in the spectrum are shown the bands at 2963 cm^{-1} and at 1438, 1198 cm^{-1} attributable to the stretching and bending vibrations of CH_3 respectively; the band at 1713 cm^{-1} due to the stretching vibrations of carbonyl C=O; the band at 1636 cm^{-1} related to the stretching vibrations of C=C and the two bands at 1304 and 882 cm^{-1} related to the stretching vibrations of the C–O ester. The bands at 989 and 899 cm^{-1} are due to the bending vibrations of the C–H groups and the signals at 773 and 671 cm^{-1} are due to C=O bending.

3.4.2 DMF-RAMEB 1:1 binary system (mol/mol)

In Figures 9 and 10, the DSC and TGA curves, respectively of DMF, RAMEB, their physical mixture (PM) 1:1 mol/mol and the products obtained by kneading (KN) were compared. The RAMEB DSC profile (Figure 9, curve b) showed a first broadened endothermic peak at about 80 °C, due to the dehydration of the sample and therefore associated in TGA analysis (Figure 10, curve b) with the loss of water molecules from the CD cavity, followed by the decomposition of the anhydrous product. For this system, an interaction was already evident following simple mixing, because of the disappearance of the DMF melting peaks from both the DSC thermal analysis of the PM (Figure 9, curve c) and the KN (Figure 9, curve d) products. This occurrence indicates high affinity between host and guest, as previously already observed in other studies (Catenacci et al., 2023; Kondoros et al., 2023).

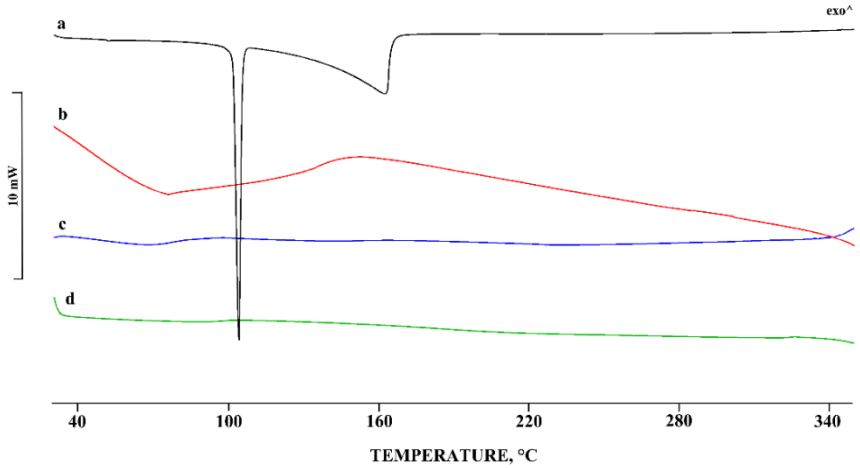

Figure 9. DSC curves of DMF (a), RAMEB (b), their physical mixture (c) and their KN product (d) in a 1:1 (mol/mol) ratio.

The TGA curves of the PM showed a first mass loss in the temperature range between 40 and 80 °C due to CD dehydration, followed by the DMF mass loss of about 64%, in the temperature range between 80 and 174 °C. The last mass loss after 280 °C was instead due to the decomposition of the remaining amount of drug and CD in the system (Figure 10). The DMF mass loss was recorded for the KN product at a temperature approximately 20 °C higher than that registered for the untreated mixture (in the range 194-274 °C) indicating a stronger interaction between the drug and CD in the KN product Both binary systems showed reduced mass losses in the temperature range of DMF decomposition, indicating the stabilizing effect of CD even in the physical mixture in agreement with the DSC results.

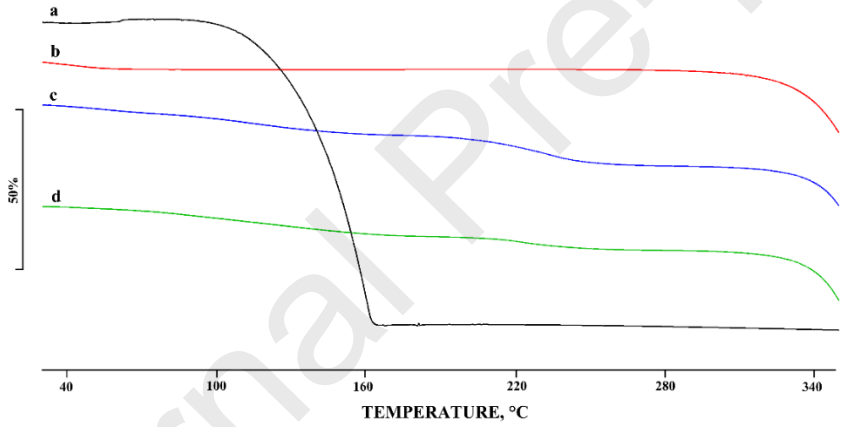

Figure 10. TGA curves of DMF (a), RAMEB (b), their physical mixture 1:1 (mol/mol) (c) and their kneaded product (d).

The thermal data were supported by FT-IR analysis. In fact, the comparison of the spectra of the starting components with those of the binary systems showed some characteristic DMF bands (in particular at 1713, 1636 and 1304 cm^{-1}) shifted to higher frequencies in the PM and KN products, as a consequence of host-guest interaction (Figure 11).

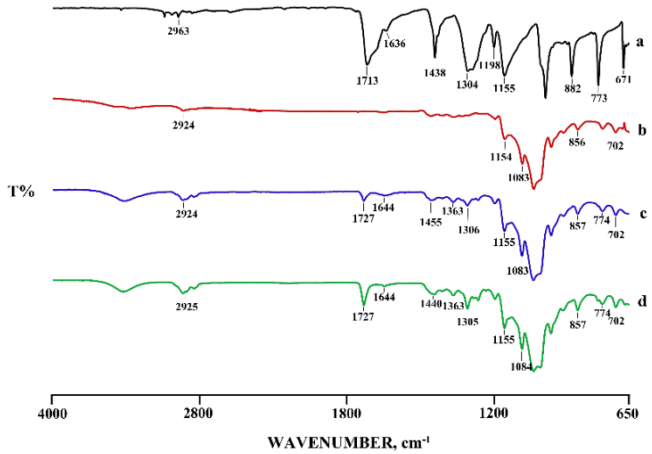

Figure 11. FT-IR spectra of DMF (a), RAMEB (b), their physical mixture 1:1 (mol/mol) (c) and their kneaded product (d).

3.4.3 DMF-RAMEB 1:2 binary system (mol/mol)

For the binary system obtained with an excess of methylated CD, the thermal and spectroscopic data were very similar to those obtained for the system with an equimolar ratio. The interaction was already evident following simple mixing, both from the thermal analysis (disappearance of the DMF melting peak, Figure 12) and the spectroscopic analysis (shift ~~at~~ to higher wavenumbers of absorption bands, Figure 13).

Furthermore, the TGA analysis has confirmed for the product DMF-RAMEB 1:2 (mol/mol), obtained by kneading, the thermal stabilization of the drug, that completely decomposed at higher temperature than the untreated DMF (curves not reported).

From thermal and spectroscopic characterization, it appears that the best interaction was achieved in the KN product with the higher molar ratio of CD.

Figure 12. DSC curves of DMF (a), RAMEB (b), their physical mixture ~~1:2 (mol/mol)~~ (c) and their kneaded product (d) in a 1:2 (mol/mol) ratio.

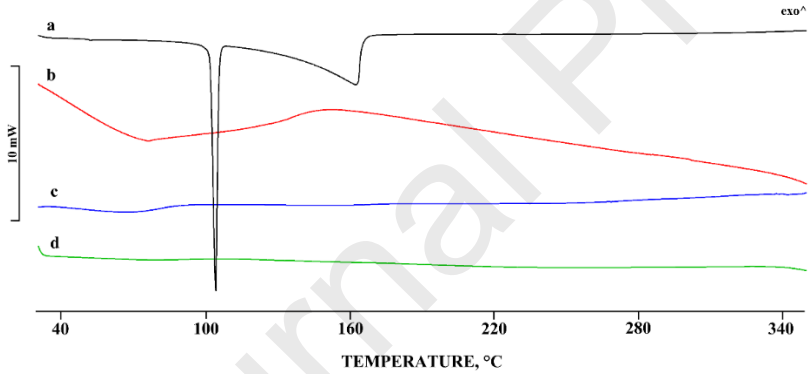

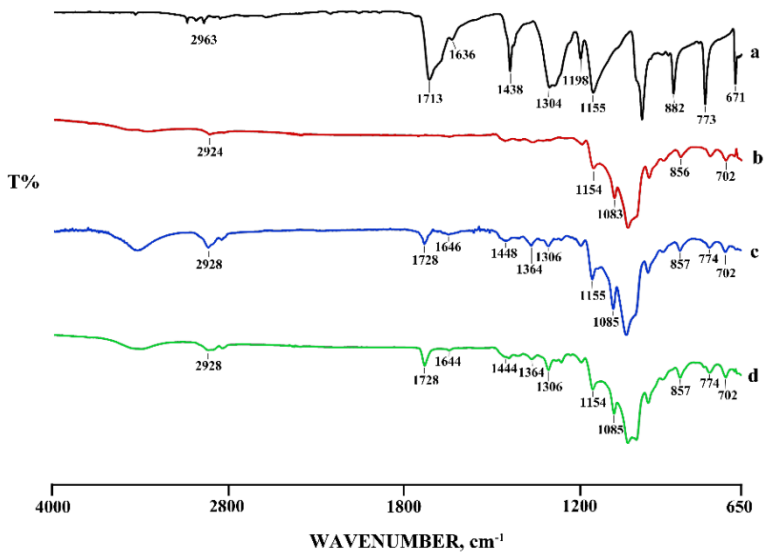

Figure 13. FT-IR spectra of DMF (a), RAMEB (b), their physical mixture 1:2 (mol/mol) (c) and their kneaded product (d).

3.4.4 PXRD analysis of DMF and its binary system

In Figure 14 the PXRD patterns of DMF, RAMEB, DMF-RAMEB physical mixture and their KN products are compared.

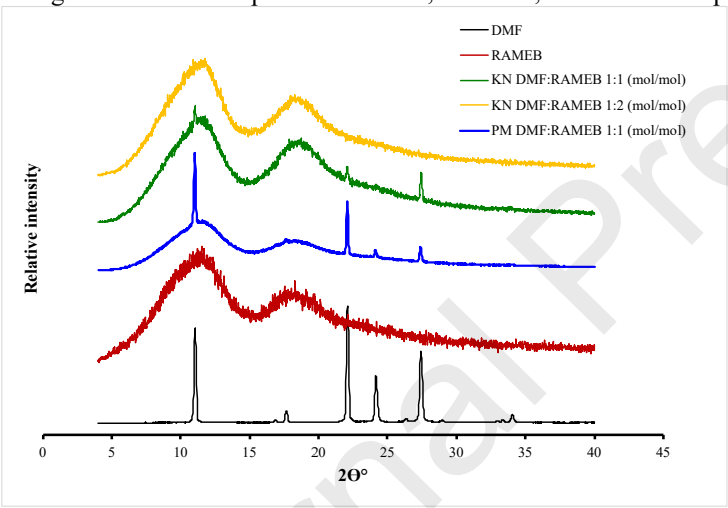

Figure 14. PXRD patterns of DMF, RAMEB, DMF-RAMEB physical mixture in a 1:1 (mol/mol) ratio and kneaded products in a 1:1 (mol/mol) and 1:2 (mol/mol) ratio, respectively.

The pattern of pure DMF (black) confirmed the crystallinity of the drug, already evidenced by thermal analysis, and it also corresponded with that calculated from the X-ray structure reported in the Cambridge Structural Database (Groom et al., 2016). The pattern of DMF-RAMEB physical mixture 1:1 (mol/mol) (blue), reported as a representative, showed the superimposed patterns of the two components, confirming the homogeneity in the binary systems. However, while the three major peaks of DMF were still evident in the pattern of the KN product DMF-RAMEB 1:1 (mol/mol) (green), even though characterized by relatively low intensities, these peaks completely disappeared in the pattern of the KN product obtained with the higher CD proportion (yellow). These results confirmed the interaction between DMF and CD, at lower extent for PM and more complete for KN products, as already seen in all the thermal analysis profiles.
~~This result~~ They moreover confirmed that, from a physicochemical characterization point of view, the best host-guest interaction was achieved with the DMF-RAMEB 1:2 (mol/mol) KN system, in accordance with the results of DoE assisted freeze drying processes. This product was therefore used for the further preparation of a nasal powder based on chitosan.

3.5 ~~Nasal~~ Powder preparation

Mucoadhesion properties of a powder can be useful to maintain it longer at the nasal mucosa site, thereby contributing to absorption enhancement. To improve the DMF-CD complex mucoadhesion, different methods of its association with chitosan, as a well-known mucoadhesive polymer, were here compared.
The first method used to obtain a chitosan-based mucoadhesive nasal powder of the DMF-CD interaction product was based on spray drying, where a solution of CS·HCl and DMF-RAMEB 1:2 complex was processed for comparison with a solution of CS·HCl and free DMF (control). Spray drying is ~~in fact~~ a first-choice preparative method for nasal powders,

as it is easily scalable and through the control of process parameters can yield microparticles of the desired dimensions and shape (Henriques et al., 2022; Jüptner and Scherliess, 2020). A CS·HCl crosslinking process based on TPP, well known in the literature since it is solvent-free and involves mild conditions, was also explored (Pan et al., 2020). The CS·HCl and DMF-CD solutions were added to TPP solution, both under intense stirring to obtain a fine suspension, and without stirring to obtain larger beads. In both cases, the suspensions were separated by centrifugation or dialysis, and a powder was then obtained by freeze drying. Finally, a plain solution of DMF-CD and CS·HCl was directly freeze dried. For all these systems, the results of the DMF recovery can be compared in Table 4, where the percentage of DMF, MMF and FA are given, referring to the total µmoles expected in the powder.

Table 4. Recovery percentage data obtained by quantifying DMF, MMF and FA for all the powders loaded with DMF-RAMEB 1:2 (mol/mol) KN product.

	Spray drying		Freeze drying		
	DMF-CS (control)	DMF-CD + CS solution	TPP CS beads	TPP CS suspension	DMF-CD + CS solution
DMF	0.08 ± 0.03	9.5 ± 2.3	7.0 ± 4.1	9.4 ± 5.1	49.9 ± 1.1
MMF	0.02 ± 0.01	3.9 ± 2.1	4.7 ± 2.5	8.6 ± 3.9	2.01 ± 0.02
FA	0.22 ± 0.02	1.00 ± 0.01	-	-	0.3 ± 0.2

As can be seen in Table 4, the spray drying method resulted in a complete loss (recovery of 0.08%) of DMF in the control sample without CD (DMF-CS). The 1:2 KN product with RAMEB conferred some protection towards the drug loss, that even in this case, however, is observed at almost 90% conceivably due to sublimation. If the MMF and FA percentages are considered in this sample, it must be noticed that they represent the 14.4% and the 6.9% of the total residual, indicating that the process conditions strongly favour hydrolysis too. Despite the improvement of the DMF stabilization that can be seen also in this case by RAMEB complexation, the spray drying method appears unsuitable as a preparative method. Temperature, air flow, and possibly partial dissociation equilibrium of the DMF-CD complex in solution can be considered responsible for this result.

Similar results, in terms of recovery of DMF, were recorded for the powder obtained by freeze drying a suspension of beads and a nanosuspension, both obtained by ionotropic gelation (Table 4).

This result can be explained by the loss in the aqueous phase, during the preparation of highly soluble DMF-RAMEB KN product, which might not be encapsulated in the CS·HCl-TPP cross-linking system.

The last preparative method investigated was the lyophilization of a solution containing the KN product and CS·HCl without cross-linking. The DMF recovery of about 50% of the theoretical amount, together with the low amount of MMF in the final product, indicate good chemical stability for this formulation, which corresponds to the best recovery of DMF and the lowest hydrolytic degradation among the tested systems. In this sample the loading capacity of the powder was also the highest, corresponding to 2.07% DMF loading in the powder, compared to 0.45% of DMF-CD powder obtained by freeze drying, while both TPP crosslinked powders resulted in a loading capacity of about 0.2%.

The dosages required for N2B delivery with respect to oral administration are quite low, ranging between 0.01% and 1% of the oral dosage (Erdo et al., 2018). Considering 50 mg as the maximum amount of powder compatible with a nasal administration (Rigaut et al., 2022), the freeze dried DMF-CD-CS·HCl sample seems the only one that can potentially deliver a therapeutically useful dose of DMF.

The images of this powder obtained from optical (A) and scanning electron microscopy (B) are given in Figure 15 and show particles with an irregular shape and highly porous structure. The particle size distribution (Figure 15 C) is in accordance with the sieving step. It is well known that the powder's particle size and morphology are critical for the nasal administration and impact. According to the literature, dimensions between 10 and 45 µm are desirable for nasal delivery (Henriques et al., 2022). However, considering the flat morphology and the high porosity of the freeze dried powder obtained here, a specific study, for example using nasal casts, will be necessary to optimize the powder properties relevant for nasal deposition.

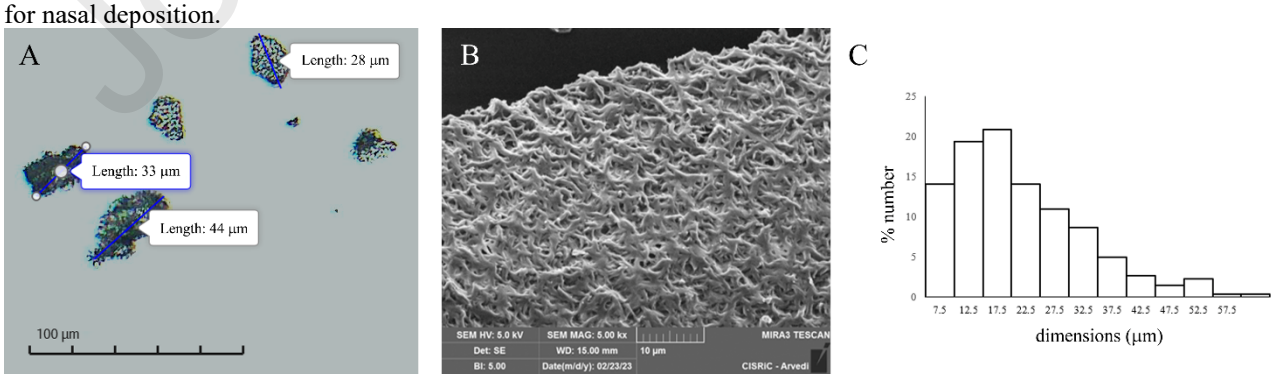

Figure 15. Optical (A), SEM (B) image and particle size analysis (C) of DMF-RAMEB CS·HCl freeze-dried powder.

Water uptake and mucoadhesion behaviour were subsequently evaluated on this freeze dried DMF-RAMEB-CS·HCl sample.

3.6 Water Uptake

The powder was able to absorb water within a few seconds of being in contact with it (Figure 16); however, the small amount of water was enough to determine the fast dissolution of the powder due to the presence of CDs, as previously demonstrated (Rassu et al., 2018; Rassu et al., 2015).

Figure 16. Water uptake capacity of the freeze dried DMF-RAMEB-CS·HCl sample.

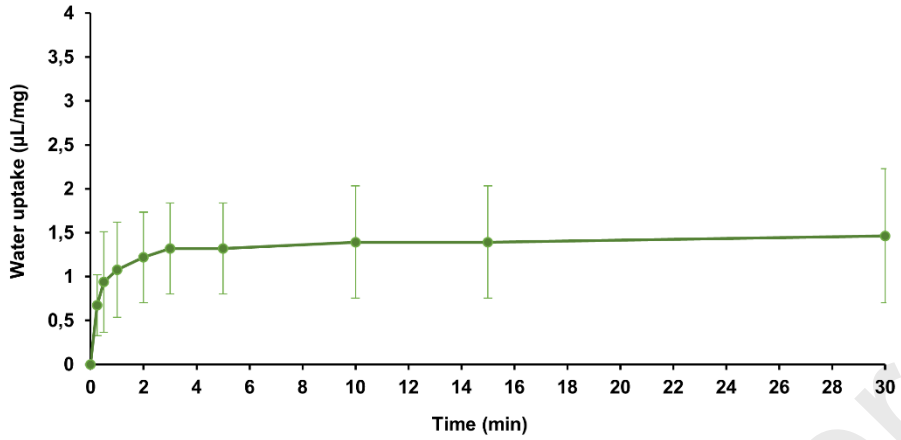

3.7 Mucoadhesion test

A mucoadhesion test was carried out on the powder resulting from the freeze drying process of the solution based on the CS·HCl and DMF-RAMEB KN product, which showed the best percentage of recovery of the active compared to the other formulations.

The mucoadhesion force, evaluated by the displacement of the powder samples on an inclined plane as a function of time, evidenced a distance covered measuring about 80% less in twice the time on the support containing mucin, as a consequence of the interaction between the positively charged groups of CS·HCl and the negatively charged groups of mucin.

It is possible to highlight a more marked solubilization effect in the case of freeze dried powder. Due to both the presence of RAMEB and the high porosity of the powder, this effect is more evident in the products placed on the support containing only agar, as a consequence of the powder's solubilization, which tends to dehydrate the surface of the plate (Figure 17).

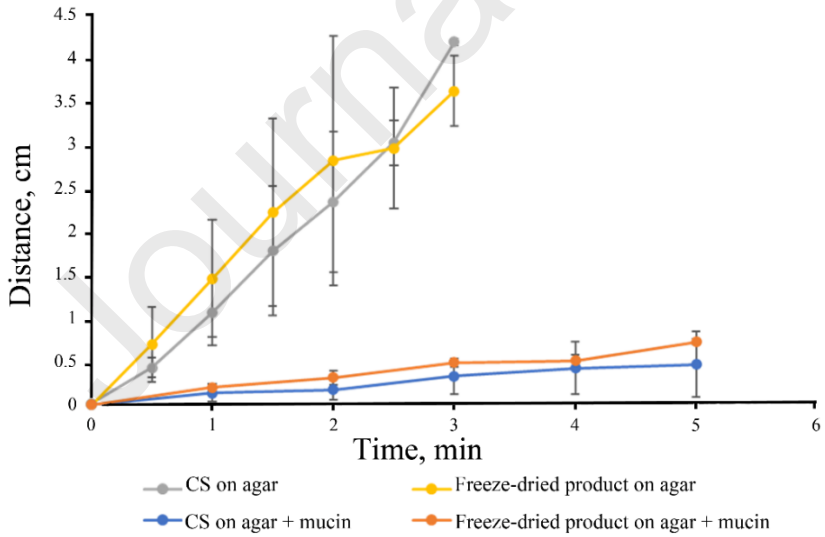

Figure 17. Time-dependent displacement of CS·HCl and freeze dried powders on agar and agar-mucin plate. Average ± SD; n=3.

The formulation showed an ex vivo mucoadhesive strength statistically different from that of the control (Figure 18) ($P = 0.045$). The very small difference in strength between the sample and the control can be explained considering the results obtained in the water uptake determination and it does not mean that the powders are not mucoadhesive. In fact, after nasal administration, due to their rapid water absorption, the powder quickly adheres and dissolves at the deposition site (Rassu et al., 2015).

This behaviour can be useful also considering the highly porous structure of the powder particles, and their flaky shape. Rapid water uptake and dissolution at the contact with mucosa should reduce the risk for the powder to be inhaled to deeper respiratory tracts, until lungs.

Figure 18. Ex vivo mucoadhesive strength.

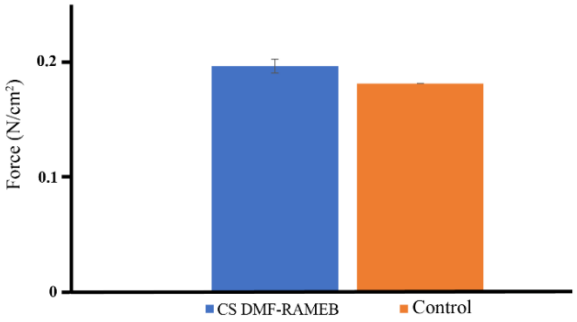

~~3~~4. CONCLUSIONS

The present work focused on the preparation and characterization of nasally administrable powder, based on the use of a binary system of the drug dimethyl fumarate (DMF) and a semisynthetic derivative of β-CD (RAMEB), since DMF proved to be highly susceptible to hydrolysis and sublimation phenomena.

DMF was combined with two amorphous highly water soluble β-CD derivatives: hydroxypropyl β-cyclodextrin (HPβCD) and methyl β-cyclodextrin (RAMEB).

Phase solubility studies were performed to determine the stability constants ($K_{1:1}$) of the DMF-HPβCD and DMF-RAMEB binary systems. It has been highlighted how the concentration of the active substance increases linearly with increasing concentration of CD, with an A_L-type profile, indicating the formation of a monomolecular complex between DMF and CD. The low value of the stability constant could be exploited as an advantage for nasal administration, where the goal is the release of the drug within a short duration of contact between the solution and mucosa, in the presence of limited quantities of physiological fluid.

The use of CDs has also demonstrated enhancements in terms of DMF stability. In fact, it has been shown that the formation of binary systems reduces the tendency of DMF to undergo hydrolysis which gives rise to MMF. In particular, the DMF-RAMEB 1:2 (mol/mol) KN product has afforded the most promising results, and this is important for the prospective use of the complex, since RAMEB is the preferred CD, according to literature studies, for nasal administration.

The interaction between the drug and this derivative of β–CD was also confirmed by thermal analysis, FT-IR spectroscopy and powder X-ray diffraction.

The present work subsequently focused on the comparison of different methods commonly used to develop a nasally administrable powder containing the API-CD binary systems. To evaluate the stability imparted to the active substance by complex formation, a freeze drying study, based on the Design of Experiment approach was conducted. The DMF-RAMEB complex in a molar ratio of 1:2 (mol/mol) showed the best stabilization of DMF and was then used as the basis to produce a dry mucoadhesive powder.

The methods employed involved the use of equipment for the production of dry powders such as spray drying and freeze drying with particular concern for the conditions involving lower DMF hydrolysis and higher mass recovery. The best results were furnished by the freeze-dried solutions of CS and complex, with the highest percentage recovery of DMF (about 50%).

The structure of the very porous powder guarantees lightness to the lyophilization, which can be considered a very functional feature for the chosen route for administration of the powder.

Finally, the mucoadhesive behaviour of the prepared powder was also confirmed. The lyophilized product tends to hydrate in a few seconds; this effect could facilitate the solubilization of the complex and therefore the possible absorption of the active through the nasal mucosa.

The use of CDs associated to freeze drying method appears to be a valid tool to overcome the problems related to stability and water solubility of the DMF~~., in view of its potential formulation in a powder for nasal application.~~ To our knowledge this is the first study on the formulation of DMF as possible powder for nasal application. Our results put in evidence that the methods normally used to produce nasal powders are not compatible with the quite poor DMF stability. The present paper suggests some strategies to overcome these formulative problems.

Starting from the results here obtained, powder dimensions and shape still must be further optimized in the perspective of nasal administration. Specific studies of deposition and release will be further necessary preliminary to in vitro biocompatibility and in vivo evaluation of DMF passage to the CNS by the N2B route.

Author Contributions: Eleonora Sofia Cama: Conceptualization, Methodology, Validation, Formal analysis, Investigation, Data curation, Writing - original draft, Visualization. **Laura Catenacci**: Conceptualization, Formal analysis, Investigation, Data curation, Resources, Writing - review & editing, Visualization. **Sara Perteghella**: Methodology, Validation, Investigation, Data curation, Formal analysis, Visualization. **Milena Sorrenti**: Conceptualization, Formal analysis, Resources, Writing - review & editing, Visualization, Supervision, Project administration, Funding acquisition. **Mino R. Caira**: Methodology, Visualization, Writing - review & editing. **Giovanna Rassu**: Investigation, Methodology, Validation, Visualization. **Elisabetta Gavini**: Methodology, Validation, Visualization. **Paolo Giunchedi**: Methodology, Validation, Visualization, Supervision. **Maria Cristina Bonferoni**: Conceptualization, Methodology, Formal analysis, Resources, Writing - review & editing, Visualization, Funding acquisition, Supervision.
All authors have read and agreed to the published version of the manuscript.

Acknowledgements: The authors wish to thank CISRiC (University of Pavia) for assistance with SEM analysis, ~~and~~ Dott. Giorgio Marrubini for providing qualified assistance with HPLC measurements and Ms Rendani Mashavhanduna for recording the PXRD patterns. Mino R. Caira thanks the University of Cape Town for access to research facilities.

Conflicts of Interest: The authors declare no conflict of interest.

Bibliography (su EndNote):

Bonferoni, M.C., Rassu, G., Gavini, E., Sorrenti, M., Catenacci, L., Giunchedi, P., 2020. Nose-to-Brain Delivery of Antioxidants as a Potential Tool for the Therapy of Neurological Diseases. Pharmaceutics 12, 21.

Catenacci, L., Sorrenti, M., Bonferoni, M.C., Hunt, L., Caira, M.R., 2020. Inclusion of the Phytoalexin trans-Resveratrol in Native Cyclodextrins: A Thermal, Spectroscopic, and X-Ray Structural Study. Molecules 25.

Catenacci, L., Vicatos, A.I., Sorrenti, M., Bonferoni, M.C., Caira, M.R., 2022. Native Cyclodextrins as Complexation Agents for Pterostilbene: Complex Preparation and Characterization in Solution and in the Solid State. Pharmaceutics 14.

Catenacci, L., Vicatos, A.I., Sorrenti, M., Edmonds-Smith, C., Bonferoni, M.C., Caira, M.R., 2023. Complexation between the Antioxidant Pterostilbene and Derivatized Cyclodextrins in the Solid State and in Aqueous Solution. Pharmaceuticals 16.

Chapman, C.D., Frey, W.H., Craft, S., Danielyan, L., Hallschmid, M., Schithöth, H.B., Benedict, C., 2013. Intranasal Treatment of Central Nervous System Dysfunction in Humans. Pharmaceutical Research 30, 2475-2484.

Colombo, M., Figueiró, F., Dias, A.D., Teixeira, H.F., Battastini, A.M.O., Koester, L.S., 2018. Kaempferol-loaded mucoadhesive nanoemulsion for intranasal administration reduces glioma growth in vitro. International Journal of Pharmaceutics 543, 214-223.

Dehghan, S., Kheiri, M.T., Tabatabaiean, M., Darzi, S., Tafaghodi, M., 2013. Dry-powder form of chitosan nanospheres containing influenza virus and adjuvants for nasal immunization. Archives of Pharmacal Research 36, 981-992.

Dello Russo, C., Scott, K.A., Pirmohamed, M., 2021. Dimethyl fumarate induced lymphopenia in multiple sclerosis: A review of the literature. Pharmacology & Therapeutics 219.

Erdo, F., Bors, L.A., Farkas, D., Bajza, A., Gizurarson, S., 2018. Evaluation of intranasal delivery route of drug administration for brain targeting. Brain Research Bulletin 143, 155-170.

Esposito, E., Cortesi, R., Drechsler, M., Fan, J., Fu, B.M., Calderan, L., Mannucci, S., Boschi, F., Nastruzzi, C., 2017. Nanoformulations for dimethyl fumarate: Physicochemical characterization and in vitro/in vivo behavior. European Journal of Pharmaceutics and Biopharmaceutics 115, 285-296.

Giunchedi, P., Gavini, E., Bonferoni, M.C., 2020. Nose-to-Brain Delivery. Pharmaceutics 12.

Goldenberg, M.M., 2012. Multiple Sclerosis Review, Pharmacy and Therapeutics, pp. 175-184.

Groom, C.R., Bruno, I.J., Lightfoot, M.P., Ward, S.C., 2016. The Cambridge Structural Database. Acta Crystallographica Section B-Structural Science Crystal Engineering and Materials 72, 171-179.

Guzowski, s.-m.a.t.Q.S.I., "inventor": "$inventor"}" class="style-scope patent-result" data-inventor="John Guzowski">John</state-modifier>, <state-modifier act="{"type": "QUERY_SEARCH_INVENTOR", i.i.c.s.-s.p.-r.d.-i.W.K.K., </state-modifier>William, <state-modifier act="{"type": "QUERY_SEARCH_INVENTOR", i.i.c.s.-s.p.-r.d.-i.E.I.I., </state-modifier>Erwin, 2016. PROCESS FOR PREPARING HIGH PURITY

AND CRYSTALLINE DIMETHYL FUMARATE. Biogen IDECMA Inc., Cambridge, MA (US), United States.

Gänger, S., Schindowski, K., 2018. Tailoring Formulations for Intranasal Nose-to-Brain Delivery: A Review on Architecture, Physico-Chemical Characteristics and Mucociliary Clearance of the Nasal Olfactory Mucosa. Pharmaceutics 10, 28.

Habib, A.A., Hammad, S.F., Amer, M.M., Kamal, A.H., 2021. Stability indicating RP-HPLC method for determination of dimethyl fumarate in presence of its main degradation products: Application to degradation kinetics. Journal of Separation Science 44.

Havrdova, E., Hutchinson, M., Kurukulasuriya, N.C., Raghupathi, K., Sweetser, M.T., Dawson, K.T., Gold, R., 2013. Oral BG-12 (dimethyl fumarate) for relapsing-remitting multiple sclerosis: a review of DEFINE and CONFIRM. Expert Opinion on Pharmacotherapy 14, 2145-2156.

Henriques, P., Fortuna, A., Doktorovova, S., 2022. Spray dried powders for nasal delivery: Process and formulation considerations. European Journal of Pharmaceutics and Biopharmaceutics 176, 1-20.

Higuchi, T., 1965. Phase-solubility techniques, in: Connors, K.A. (Ed.), Advances in Analytical Chemistry and Instrumentation, pp. 117-212.

Jansook, P., Ogawa, N., Loftsson, T., 2018. Cyclodextrins: structure, physicochemical properties and pharmaceutical applications. International Journal of Pharmaceutics 535, 272-284.

Jarudilokkul, S., Tongthammachat, A., Boonamnuayvittaya, V., 2011. Preparation of chitosan nanoparticles for encapsulation and release of protein. Korean Journal of Chemical Engineering 28, 1247-1251.

Juliano, C., Cossu, M., Pigozzi, P., Rassu, G., Giunchedi, P., 2008. Preparation, In Vitro Characterization and Preliminary In Vivo Evaluation of Buccal Polymeric Films Containing Chlorhexidine. Aaps Pharmscitech 9, 1153-1158.

Jüptner, A., Scherliess, R., 2020. Spray Dried Formulations for Inhalation-Meaningful Characterisation of Powder Properties. Pharmaceutics 12, 15.

Kawakami, T., Isama, K., Matsuoka, A., Nishimura, T., 2011. Determination of Dimethyl Fumarate and Other Fumaric and Maleic Acid Diesters in Desiccants and Consumer Products in Japan. Journal of Health Science 57, 236-244.

Kim, B.G., Kim, J.H., Kim, S.W., Jin, K.S., Cho, J.H., Kang, J.M., Park, S.Y., 2013. Nasal pH in patients with chronic rhinosinusitis before and after endoscopic sinus surgery. American Journal of Otolaryngology 34, 505-507.

Kondoros, B.A., Kókai, D., Burián, K., Sorrenti, M., Catenacci, L., Csóka, I., Ambrus, R., 2023. Ternary cyclodextrin systems of terbinafine hydrochloride inclusion complexes: Solventless preparation, solid-state, and in vitro characterization. Heliyon 9, 13.

Linker, R.A., Gold, R., 2013. Dimethyl Fumarate for Treatment of Multiple Sclerosis: Mechanism of Action, Effectiveness, and Side Effects. Current Neurology and Neuroscience Reports 13.

Linker, R.A., Haghikia, A., 2016. Dimethyl fumarate in multiple sclerosis: latest developments, evidence and place in therapy. Therapeutic Advances in Chronic Disease 7, 198-207.

Luppi, B., Bigucci, F., Corace, G., Delucca, A., Cerchiara, T., Sorrenti, M., Catenacci, L., Di Pietra, A.M., Zecchi, V., 2011. Albumin nanoparticles carrying cyclodextrins for nasal delivery of the anti-Alzheimer drug tacrine. European Journal of Pharmaceutical Sciences 44, 559-565.

Manta, K., Papakyriakopoulou, P., Chountoulesi, M., Diamantis, D.A., Spaneas, D., Vakali, V., Naziris, N., Chatziathanasiadou, M.V., Andreadelis, I., Moschovou, K., Athanasiadou, I., Dallas, P., Rekkas, D.M.,

Demetzos, C., Colombo, G., Banella, S., Javornik, U., Plavec, J., Mavromoustakos, T., Tzakos, A.G., Valsami, G., 2020. Preparation and Biophysical Characterization of Quercetin Inclusion Complexes with β-Cyclodextrin Derivatives to be Formulated as Possible Nose-to-Brain Quercetin Delivery Systems. Molecular Pharmaceutics 17, 4241-4255.

Mazancová, P., Némethová, V., Trel'ová, D., Klescíková, L., Lacík, I., Rázga, F., 2018. Dissociation of chitosan/tripolyphosphate complexes into separate components upon pH elevation. Carbohydrate Polymers 192, 104-110.

McGinley, M.P., Goldschmidt, C.H., Rae-Grant, A.D., 2021. Diagnosis and Treatment of Multiple Sclerosis: A Review (vol 325, pg 765, 2021). Jama-Journal of the American Medical Association 325, 2211-2211.

Mrowietz, U., Szepietowski, J.C., Loewe, R., van de Kerkhof, P., Lamarca, R., Ocker, W.G., Tebbs, V.M., Pau-Charles, I., 2017. Efficacy and safety of LAS41008 (dimethyl fumarate) in adults with moderate-to-severe chronic plaque psoriasis: a randomized, double-blind, Fumaderm® - and placebo-controlled trial (BRIDGE). British Journal of Dermatology 176, 615-623.

Mukesh, S., Kumar , Annika, S., 2021. Particle size analysis, in: Mukesh, Kumar Singh, A.S. (Eds.), Characterization of Polymers and Fibres, pp. 341-358.

Mwema, A., Muccioli, G.G., des Rieux, A., 2023. Innovative drug delivery strategies to the CNS for the treatment of multiple sclerosis. Journal of Controlled Release 364, 435-457.

Pan, C.L., Qian, J.Q., Zhao, C.Y., Yang, H.Y., Zhao, X.H., Guo, H., 2020. Study on the relationship between crosslinking degree and properties of TPP crosslinked chitosan nanoparticles. Carbohydrate Polymers 241, 9.

Popielec, A., Loftsson, T., 2017. Effects of cyclodextrins on the chemical stability of drugs. International Journal of Pharmaceutics 531, 532-542.

Rassu, G., Ferraro, L., Pavan, B., Giunchedi, P., Gavini, E., Dalpiaz, A., 2018. The Role of Combined Penetration Enhancers in Nasal Microspheres on In Vivo Drug Bioavailability. Pharmaceutics 10.

Rassu, G., Soddu, E., Cossu, M., Brundu, A., Cerri, G., Marchetti, N., Ferraro, L., Regan, R.F., Giunchedi, P., Gavini, E., Dalpiaz, A., 2015. Solid microparticles based on chitosan or methyl-β-cyclodextrin: A first formulative approach to increase the nose-to-brain transport of deferoxamine mesylate. Journal of Controlled Release 201, 68-77.

Rassu, G., Sorrenti, M., Catenacci, L., Pavan, B., Ferraro, L., Gavini, E., Bonferoni, M.C., Giunchedi, P., Dalpiaz, A., 2021. Versatile Nasal Application of Cyclodextrins: Excipients and/or Actives? Pharmaceutics 13.

Rigaut, C., Deruyver, L., Goole, J., Haut, B., Lambert, P., 2022. Instillation of a Dry Powder in Nasal Casts: Parameters Influencing the Olfactory Deposition With Uni- and Bi-Directional Devices. Frontiers in Medical Technology 4, 17.

Schneider, C.A., Rasband, W.S., Eliceiri, K.W., 2012. NIH Image to ImageJ: 25 years of image analysis. Nature Methods 9, 671-675.

Trenkel, M., Scherliess, R., 2021. Nasal Powder Formulations: In-Vitro Characterisation of the Impact of Powders on Nasal Residence Time and Sensory Effects. Pharmaceutics 13.

Truzzi, E., Rustichelli, C., de Oliveira, E.R., Ferraro, L., Maretti, E., Graziani, D., Botti, G., Beggiato, S., Iannuccelli, V., Lima, E.M., Dalpiaz, A., Leo, E., 2021. Nasal biocompatible powder of Geraniol oil complexed with cyclodextrins for neurodegenerative diseases: physicochemical characterization and in vivo evidences of nose to brain delivery. Journal of Controlled Release 335, 191-202.

Wilson, B., Alobaid, B.N.M., Geetha, K.M., Jenita, J.L., 2021. Chitosan nanoparticles to enhance nasal absorption and brain targeting of sitagliptin to treat Alzheimer's disease. Journal of Drug Delivery Science and Technology 61.

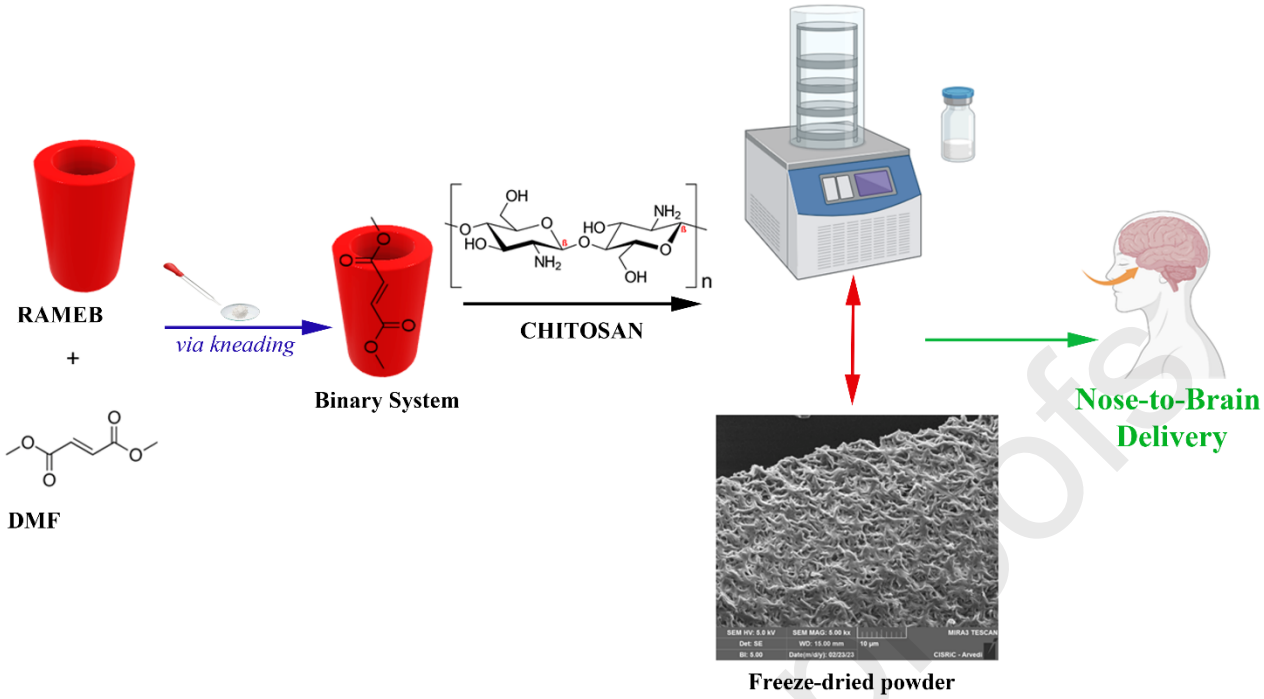

Declaration of interests

☒ The authors declare that they have no known competing financial interests or personal relationships that could have appeared to influence the work reported in this paper.

☐ The authors declare the following financial interests/personal relationships which may be considered as potential competing interests: